Two-Dimensional Linear Drive Combined with Electromagnetic Levitation for a Flexible Transportation Line

T. Koseki, Y. Makino, and J. Liu
Department of Electrical Engineering
The University of Tokyo
7-3-1 Hongo, Bunkyo-Ku, Tokyo, Japan
Tel: +81-3-5841-6676 Fax: +81-3-5800-5988
Email: makino@koseki.t.u-tokyo.ac.jp

S. Inui, and Y. Ohira
Department of Electrical and Electronic Engineering
College of Engineering
Nihon University
Email: inui@ee.ce.nihon-u.ac.jp

***Abstract*—The combination of electromagnetic suspension and linear motor has been widely used in many industrial fields because of its advantages. A mover that has 3 electromagnets and 3 linear induction motors is proposed in this paper. It can control 6 degrees of freedom and its stator can be simple. Decentralized control and centralized controls are proposed for levitation control of 3 degrees of freedom and they are compared in simulation. Then, the advantages of centralized control have been verified.**

***Key words*—Linear induction motor, Electromagnetic suspension, Decentralized control, Centralized control**

1. INTRODUCTION

Electromagnetic suspension technology (EMS), in which attractive forces between electromagnets and ferromagnetic materials are utilized as suspension forces, is commonly used in the field of passenger transport vehicles, tool machines, frictionless bearings and conveyor systems, because of its various advantages, such as, no friction, no abrasion, low noise and small vibration, *etc*. Linear motor can generate thrust without gears, which is called a direct drive. The combination of EMS and linear motor is very useful in the conveyance systems, but its movement is usually limited to one dimension.

In order to realize more flexible conveyance system, we have proposed the coordination of a 4-pole shaped hybrid electromagnet and two-dimensional linear synchronous motor. This structure is shown in figure 1. 4-pole shaped hybrid magnet can control 3 degrees of freedom of a mover with zero power control, and two-dimensional linear synchronous motor uses 4-pole permanent magnet as its field magnet. In the experiment, it is confirmed that this coordination can realize two-dimensional conveyance system [1]. However, it has some disadvantages, such as its lack of damping in the yawing direction and complexity of its stator.

In order to overcome these disadvantages, we propose a mover that has 3 U-shaped electromagnets and 3 linear induction motors (LIMs). In this configuration, which is shown in figure 2, 6 degrees of freedom of the mover can be controlled and the stator is simply composed of iron and conductor plate.

Simulation results of 6 degrees of freedom control will be reported in this paper.

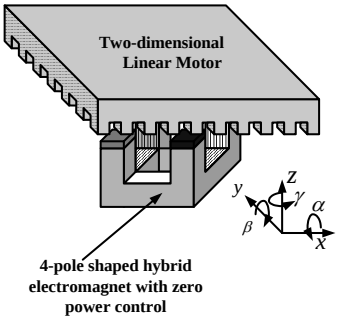

Figure 1. Coordination of 4-pole electromagnet and two-dimensional linear motor

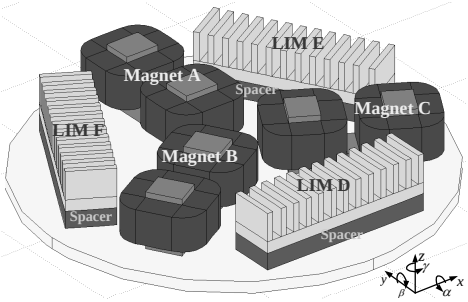

Figure 2. Configuration of the proposed mover

2. SYSTEM CONFIGURATION

2.1. *Characteristics of a LIM*

The structure of the LIM, which we are going to use in the experiment, is shown in figure 3. Firstly, we have calculated fundamental characteristics of thrust F_t and normal force F_n when the current amplitude i_s is 3.0[A], using a two-dimensional FEM program.

The characteristics of slip frequency *sf*, air gap length $g_{al} - F_t$ and *sf*, $g_{al} - F_n$ are shown in figure 4 and figure 5 respectively. From the results, thrust increase in proportion to *sf* in the region of low slip frequency. Both of thrust and normal force decrease as the gaplength increases. These characteristics are approximately described as following equations. g_{el} is effective gap length of LIM (g_{al} + thickness of secondary conductor), K_t and T_{rt} are the coefficients of thrust, K_n and T_{rn} are the coefficients of normal force.

$$F_t = \frac{K_t}{g_{el}^{1.68}} \frac{sf\, i_s^2}{1+(sf\, T_{rt})^2} \tag{1}$$

$$F_n = \frac{K_n}{g_{el}^{1.85}} \frac{i_s^2}{1+(sf\, T_{rn})^2} \tag{2}$$

In a steady state, we are using normal force of LIMs to partially suspend mover's mass. In terms of suspension and propulsion, we prefer small gap length to get large attractive force and thrust. But the smaller gap length becomes, the smaller the range of motion becomes. In order to keep sufficient range of motion and obtain normal force and thrust large enough, we have determined the air gap length to 4.0[mm].

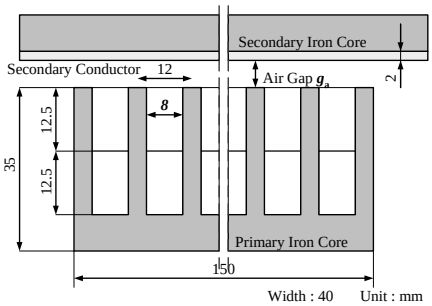

Figure 3. Configuration of a LIM

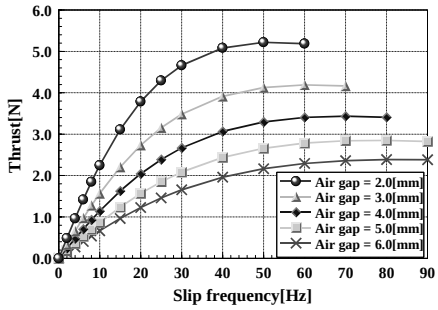

Figure 4. Characteristics of slip frequency, gap length – thrust

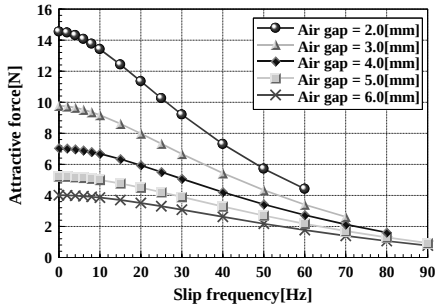

Figure 5. Characteristics of slip frequency, gap length – normal force

2.2. Control Method of a LIM

The speed of the mover will not be so high (~0.2[m/s]) and slip frequency may be low in prospective experiments. We, therefore, simply adopt slip frequency control as a control method of a LIM because thrust increases in proportion to slip frequency in the region of low slip frequency. Approximated linearized thrust equation is described as follow, and block diagram of x, y, γ control is shown in figure 6.

$$F_t \approx \frac{K_t}{g_{el}^{1.68}} i_s^2 sf \tag{3}$$

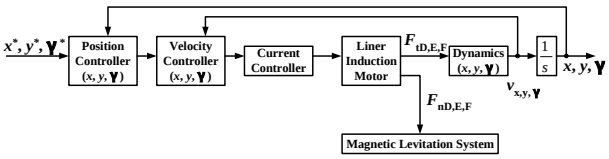

Figure 6. Block diagram of x, y, γ control

2.3. Characteristics of Electromagnet

The relationship between the current i, effective gaplength g_{ee} (air gap + thickness of secondary conductor) of electromagnet and attractive force f_m has been calculated based on a simple magnetic circuit analysis. k is an attractive force coefficient. The equation is described as follow.

$$f_m = k\left(\frac{i}{g_{ee}}\right)^2 \tag{4}$$

3. LEVITATION CONTROL METHODS

As methods to control the posture of mover, decentralized and centralized controls are described in this section. In the decentralized control, each of electromagnets control its gap length suspending one-third of total mass. In the centralized control, total posture (z, α , β) is controlled using coordinates transformation which includes the location of electromagnets. The location of electromagnets and LIMs is shown in figure 7. l_e is the distance between the centre of mover and electromagnet, l_l is the one between the centre of mover and LIM.

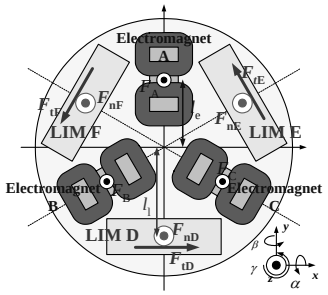

Figure 7. Location of electromagnets and LIMs

3.1. Decentralized Control

When each electromagnet suspends one-third of total mass, dynamic equations of motions including normal force of a LIM and circuit equation are described as follows. Here, M is the total mass of mover, g_A is the effective gap length of electromagnet A, g is gravitational acceleration, L is an electromagnet's inductance and R_0 is an electromagnet's resistance.

$$\frac{M}{3}\frac{d^2 g_A}{dt^2} = \frac{Mg}{3} - k\left(\frac{i_A}{g_A}\right)^2 - F_n + f_d \tag{5}$$

$$e_A = \frac{d(Li_A)}{dt} + R_0 i_A \tag{6}$$

Equations (5) and (6) are linearized around the nominal operating point $(i_A, g_A) = (I_0, g_0)$, which is decided with the following equation.

$$k\left(\frac{I_0}{g_0}\right)^2 = \frac{Mg}{3} \tag{7}$$

The linearized equations are described as follows. L_0 is an electromagnet's inductance at nominal point.

$$\frac{M}{3}s^2\Delta g_A = -K_A\Delta i_A + (K_B + K_c)\Delta g_A \tag{8}$$
$$K_A = \frac{\partial f_m}{\partial i}\Big|_{(I_0,g_0)}, K_B = -\frac{\partial f_m}{\partial g_{ee}}\Big|_{(I_0,g_0)}, K_C = -\frac{\partial f_n}{\partial g_{el}}$$

$$\Delta e_A = R_0\Delta i_A + L_0 s\Delta i_A - V_{e0}I_0 v_{g_A} \tag{9}$$
$$V_{e0} = \frac{\mu_0 N^2 S}{2{g_0}^2}$$

The controller is realized based on this linearized model as the state feedback including the integral of gap length. The controller output, which is the voltage of electromagnet, is described as follow.

$$\Delta e_A = -K_{pg}\Delta g_A - K_{dg}s\Delta g_A - K_{Iig}\Delta i_A + K_{ig}(\Delta g_A^* - \Delta g_A)/s \tag{10}$$

The transfer function from gap length command to real gap length becomes as follows.

$$\frac{\Delta g_A}{\Delta g_A^*} = \frac{a_{g0}}{a_{g4}s^4 + a_{g3}s^3 + a_{g2}s^2 + a_{g1}s^1 + a_{g0}}, \text{where}$$
$$a_{g4} = ML_0, a_{g3} = M(R_0 + K_{Iig}),$$
$$a_{g2} = -3K_A(K_{dg} - V_{e0}I_0) - 3(K_B + K_c)L_0,$$
$$a_{g1} = -3K_AK_{pg} - 3(K_B + K_c)(R_0 + K_{Iig}) \text{ and } a_{g0} = -3K_AK_{ig}. \tag{11}$$

The controller's gains are determined according to Kessler's canonical form.

$$\frac{a_{g1}}{a_{g0}} = \tau = 0.04, \frac{a_{g3}^2}{a_{g4}a_{g2}} = \frac{a_{g2}^2}{a_{g3}a_{g1}} = \frac{a_{g1}^2}{a_{g2}a_{g0}} = 2 \tag{12}$$

The controllers of electromagnet B and C are designed, as is the case with electromagnet A. The block diagram of decentralized control is shown in figure 8.

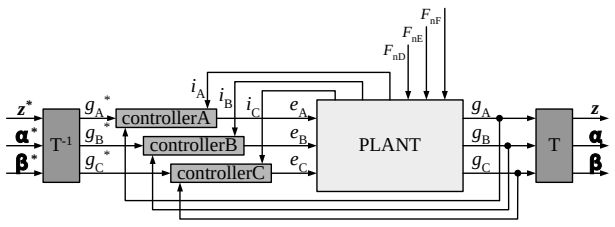

Figure 8. Block diagram of decentralized control

3.2. Centralized Control

Centralized control uses coordinates transformation to change gap length and currents of electromagnets to posture (z, α, β) and virtual currents (i_z, i_α, i_β). These coordinates transformation are described as follows.

$$\begin{pmatrix}\Delta z\\ \Delta\alpha\\ \Delta\beta\end{pmatrix} = \begin{pmatrix}-1/3 & -1/3 & -1/3\\ -2/3l_e & 1/3l_e & 1/3l_e\\ 0 & -1/\sqrt{3}l_e & 1/\sqrt{3}l_e\end{pmatrix}\begin{pmatrix}\Delta g_A\\ \Delta g_B\\ \Delta g_C\end{pmatrix} = T\begin{pmatrix}\Delta g_A\\ \Delta g_B\\ \Delta g_C\end{pmatrix} \tag{13}$$

$$\begin{pmatrix}\Delta i_z\\ \Delta i_\alpha\\ \Delta i_\beta\end{pmatrix} = \begin{pmatrix}1 & 1 & 1\\ 1 & -1/2 & -1/2\\ 0 & \sqrt{3}/2 & -\sqrt{3}/2\end{pmatrix}\begin{pmatrix}\Delta i_A\\ \Delta i_B\\ \Delta i_C\end{pmatrix} = H\begin{pmatrix}\Delta i_A\\ \Delta i_B\\ \Delta i_C\end{pmatrix} \tag{14}$$

Using these virtual variables, dynamic equations of motions are described as follows. J_α is an inertia moment of α - rotation, J_β is an inertia moment of β - rotation.

$$M\frac{d^2}{dt^2}z = F_A + F_B + F_C + F_{nD} + F_{nE} + F_{nF} - Mg - F_{dz}$$
$$J_\alpha\frac{d^2}{dt^2}\alpha = l_eF_A - \frac{l_e}{2}(F_B + F_C) - l_lF_{nD} + \frac{l_l}{2}(F_{nE} + F_{nF}) - T_{d\alpha}$$
$$J_\beta\frac{d^2}{dt^2}\beta = \frac{\sqrt{3}}{2}l_e(F_B - F_C) + \frac{\sqrt{3}}{2}l_l(F_{nF} - F_{nE}) - T_{d\beta} \tag{15}$$

When these equations are linearized, as is the case with decentralized control, linearized equations are described as follows.

$$Ms^2\Delta z = K_A\Delta i_z + 3(K_B + K_C)\Delta z$$
$$J_\alpha s^2\Delta\alpha = l_eK_A\Delta i_\alpha + \frac{3}{2}(l_e^2K_B + l_l^2K_C)\Delta\alpha \tag{16}$$
$$J_\beta s^2\Delta\beta = l_eK_A\Delta i_\beta + \frac{3}{2}(l_e^2K_B + l_l^2K_C)\Delta\beta$$
$$\Delta e_z = R_0\Delta i_z + L_0 s\Delta i_z + 3V_{e0}I_0 v_z$$
$$\Delta e_\alpha = R_0\Delta i_\alpha + L_0 s\Delta i_\alpha + \frac{3}{2}l_eV_{e0}I_0\omega_\alpha \tag{17}$$
$$\Delta e_\beta = R_0\Delta i_\beta + L_0 s\Delta i_\beta + \frac{3}{2}l_eV_{e0}I_0\omega_\beta$$

The controllers are designed in each direction assuming these equations are realized independently. The block diagram of centralized control is shown in figure 9.

$$\Delta e_z = -K_{pz}\Delta z - K_{dz}s\Delta z - K_{Iiz}\Delta i_z + K_{iz}(\Delta z^* - \Delta z)/s$$
$$\Delta e_\alpha = -K_{p\alpha}\Delta\alpha - K_{d\alpha}s\Delta\alpha - K_{Ii\alpha}\Delta i_\alpha + K_{i\alpha}(\Delta\alpha^* - \Delta\alpha)/s \tag{18}$$
$$\Delta e_\beta = -K_{p\beta}\Delta\beta - K_{d\beta}s\Delta\beta - K_{Ii\beta}\Delta i_\beta + K_{i\beta}(\Delta\beta^* - \Delta\beta)/s$$

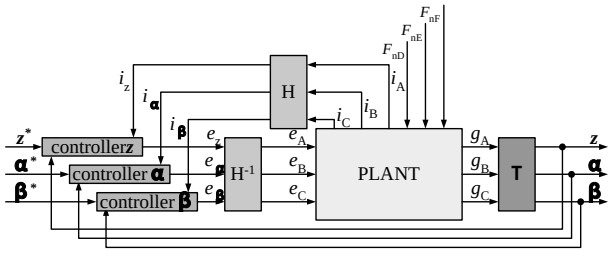

Figure 9. Block diagram of centralized control

4. SIMULATION OF 6 DEGREES OF FREEDOM CONTROL

4.1. Simulation Conditions

The parameters used in simulation of 6 degrees of freedom control are described in table 1. Initial position (z_0, α_0, β_0) is (-0.003,0,0). Simulation flow is as follows:

Time = 0[s] : Levitation starts.

Time = 1[s] : Currents are given to LIMs.

Time = 2[s] : α –rotation disturbance torque(1.28[Nm]) is given.

Time = 3[s] : (x_{ref}, y_{ref}, γ_{ref}) changes from (0,0,0) to (0.1,0.2,0).

Time = 8[s] : Simulation ends.

TABLE 1. SIMULATION CONDITIONS

M	10.4[kg]	l_e	0.090[m]
J_α	0.0726[kgm^2]	l_l	0.125[m]
J_β	0.0712[kgm^2]	k	0.0000923[Nm^2/A^2]
g_0	0.0080[m]	L_0	0.02080[H]
I_0	4.44[A]	R_0	2.00[Ω]

4.2. Simulation Results

The simulation results of six degrees of freedom control in decentralized control are shown in figure 10-12 and the ones in centralized control are shown in figure 13-15. From the results, response of α , β -rotation tends to become more unstable in the decentralized control than in the centralized control because we cannot design the controller of α , β –rotation.

The response against α –rotation disturbance depends on l_e. The simulation results are shown in figure 16-21. The results show that, the further electromagnets are placed from centre of mover, the more stable α , β –rotation response against disturbance becomes in the decentralized control, whereas the response in the centralized control is kept identical even when l_e changes.

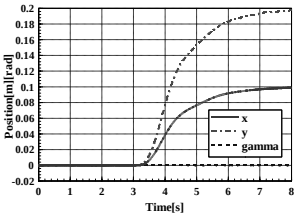

Figure 10. Position (x, y, γ) (Decentralized control)

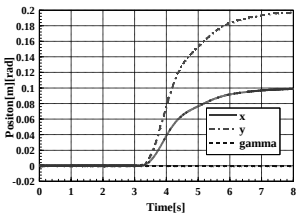

Figure 13. Position (x, y, γ) (Centralized control)

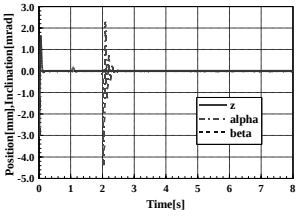

Figure 11. Posture (z, α , β) (Decentralized control)

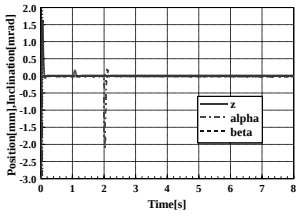

Figure 14. Posture (z, α , β) (Centralized control)

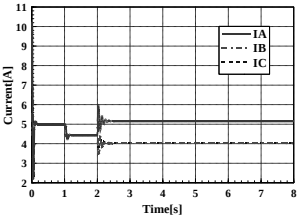

Figure 12. Current (i_A, i_B, i_C) (Decentralized control)

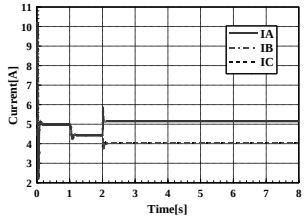

Figure 15. Current (i_A, i_B, i_C) (Centralized control)

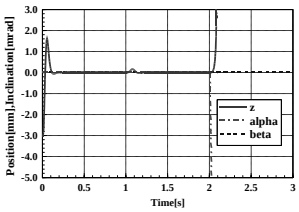

Figure 16. Posture (z, α , β) (Decentralized control) l_e=0.045

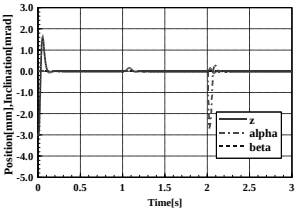

Figure 19. Posture (z, α , β) (Centralized control) l_e=0.045

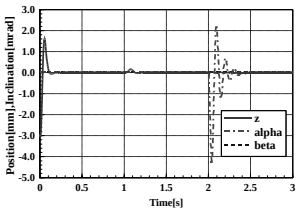

Figure 17. Posture (z, α , β) (Decentralized control) l_e=0.090

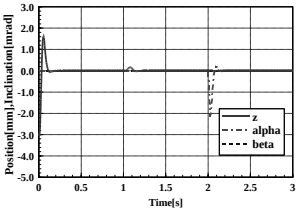

Figure 20. Posture (z, α , β) (Centralized control) l_e=0.090

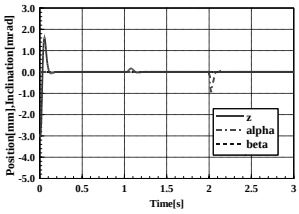

Figure 18. Posture (z, α , β) (Decentralized control) l_e=0.180

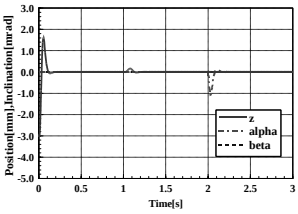

Figure 21. Posture (z, α , β) (Centralized control) l_e=0.180

5. CONCLUSIONS AND FUTURE WORKS

In this paper, the structure of a mover that has 3 LIMs and 3 electromagnets to control 6 degrees of freedom was proposed for a flexible contactless conveyance system. The decentralized and the centralized controls were proposed as methods of its levitation control, and both were compared in the simulations. From the results of the simulations, inclination tends to be unstable in the decentralized control and its stability depends on l_e.

We are going to make experiments of this system. Two dimensional position sensing is a serious problem in the two-dimensional conveyance system. We are adopting visual sensing technology, which use a few cameras to detect the position as a solution. Since usual digital camera does not have high sampling time, we are going to apply multirate sampling observer, which can guarantee precise position detection and control even with a low sampling rate of a position sensor [2].

REFERENCES

[1] J. Liu, T. Koseki, S. Inui, Y. Ohira, “The 2-Dimensional LSM Drive Experiments with 4-Pole 3 Degree-of-Freedom Maglev Control Electromagnet” IEEJ Technical Meeting on Linear Drives LD-02-83.

[2] L. Kovudhikulrungsri, T. Koseki, “PERFORMANCE IMPROVEMENT OF A LINEAR ENCODER BY MULTIRATE SAMPLING OBSERVER” LDIA2003 MI-07